Altered Activation Patterns within the Olfactory Network in Parkinson's Disease

Carolin Moessnang[1,2], Gabriele Frank[1], Ulrich Bogdahn[3], Jurgen Winkler[3,4], Mark W. Greenlee[1] and Jochen Klucken[3,4]

[1]Department of Experimental Psychology, University of Regensburg, 93053 Regensburg, Germany, [2]Rheinisch-Westfälische Technische Hochschule Aachen University, 52074 Aachen, Germany, [3]Department of Neurology, University of Regensburg, 93053 Regensburg, Germany and [4]Division of Molecular Neurology, University Hospital Erlangen, 91012 Erlangen, Germany

Address correspondence to Mark W. Greenlee. Email: mark.greenlee@psychologie.uni-regensburg.de.

Olfactory impairment is a consistent premotor symptom in sporadic Parkinson's disease (PD), presumably caused by pathological processes in the olfactory bulb and olfactory structures within mesolimbic brain areas. The objective of the present study was to obtain an in-depth insight into olfactory network dysfunction in PD patients. Event-related functional magnetic resonance imaging (3 T) was conducted with 16 early-stage PD patients and 16 matched controls during an odor detection task. Activation within the olfactory network was analyzed both in terms of strength of activation (whole-brain random effects, regions of interest [ROI] analysis based on the hemodynamic response function) as well as time-course characteristics (finite impulse response–based ROI analysis). Olfactory-induced activation in patients with PD in comparison to a standard activation pattern obtained from controls revealed profound hyperactivation in piriform and orbitofrontal cortices. However, whereas orbitofrontal areas seem to be unable to discriminate between signal and noise, primary olfactory cortex shows preserved discriminatory ability. These results support a complex network dysfunction that exceeds structural pathology observed in the olfactory bulb and mesolimbic cortices and thus demonstrate the important contribution of functional data to describe network dynamics occurring in the degenerating brain.

Keywords: cortical reorganization, fMRI, neural networks, olfaction, PD

Introduction

A very early and consistent symptom in sporadic Parkinson's disease (PD) is olfactory impairment. Indeed, early involvement of olfactory structures in the pathological process of PD is associated with olfactory dysfunction (Braak et al. 2004; Doty 2008; Zaccai et al. 2008). Thus, the characterization of olfactory functional brain activation may promote diagnostic sensitivity for detecting the premotor phase of PD. However, only a few studies have examined functional olfactory activation in PD patients so far (Westermann et al. 2008; Welge-Lussen et al. 2009). Whereas these studies rather conducted regional analyses on functional activation within frontostriatal loops associated with the olfactory task, the present study aims to investigate alterations in olfactory information processing by analyzing local activation patterns in distinct, predefined parts of the olfactory network, using functional magnetic resonance imaging (fMRI). More precisely, we hypothesized that the impact of pathology on olfactory structures will be 2-fold (Palop et al. 2006); mesolimbic olfactory brain regions that are directly affected by degenerative processes are expected to be impaired with respect to information processing and hence to display hypoactivation compared with controls (Fig. 1). These include primary (piriform cortex, entorhinal cortex, and amygdala) as well as secondary olfactory structures (para-

hippocampal cortex and hippocampus). In contrast, non-mesolimbic olfactory brain regions (insula and orbitofrontal cortices [OFCs]) are assumed to show increased activation in PD patients compared with controls, reflecting a compensatory upregulation of olfactory information processing in order to compensate network dysfunction.

Materials and Methods

Study population

Sixteen early-stage PD patients (8 women, 58.4 + 9.5 years) and 16 controls (8 women, 57.4 + 7.4 years) were recruited for the present study (for detailed sample characteristics, see Supplementary Table s1). Statistical analysis by means of a nonparametric Mann–Whitney U test confirmed successful matching of the 2 samples. None of the demographic variables differed significantly between both groups ($P_{age} = 0.616$, $P_{gender} = 1.000$, $P_{handedness} = 0.224$, $P_{verbal intelligence} = 0.239$, $P_{education} = 0.119$). None of the subjects displayed significant cognitive impairment as confirmed by a psychopathological screening using the Mini-Mental State Examination (Folstein et al. 1975). Depression was excluded using the Beck Depression Inventory (Beck et al. 1961).

Exclusion criteria leading to impaired olfactory functioning or to structural and/or functional changes in the brain encompassed acute or chronic disorders in the maxillary or frontal sinus (e.g., cold), allergies, smoking, neurological disorders (except PD for the patient group), psychiatric disorders, intake of psychoactive substances, and medication influencing olfaction. PD was diagnosed according to the guidelines of the German Society of Neurology that are based on the UK Parkinson's Disease Society Brain Bank Diagnostic Criteria for PD (Gelb et al. 1999). Patients' disease duration averaged 5.8 + 3.9 years, with Unified Parkinson Disease Rating Scale part III scores (Fahn and Elton 1987) ranging from 1 to 11.5/56 (mean score: 8 + 3.9) and Hoehn and Yahr stages ranging from I ($n = 6$), I–II ($n = 2$), and II ($n = 8$) (Hoehn and Yahr 2001). With regard to the affected side, the majority displayed right-sided parkinsonism, with only 4 patients being more affected on the left side. Symptoms could be classified as tremor-dominant in 7 patients, as akinetic-rigid in 6 patients, and as equivalent in 3 patients. All but one patient were treated with dopaminergic drugs. Equivalence dose rates ranged from 150 to 800 mg, with an average dose of 416 mg (standard deviation = 223.7 mg). The study protocol was approved by the institutional review board and conducted according to the Code of Ethical Principles for Medical Research involving human subjects of the World Medical Association (Declaration of Helsinki). All subjects gave written informed consent.

Psychophysical Assessment of Olfactory Function

Olfactory performance was quantitatively assessed using 3 subtests (sensitivity, identification, and discrimination) of the Sniffin' Sticks test (Burghardt medical technology) (Kobal et al. 1996). Individual scores of each subtest ranging from 0 (minimal performance) to 16 (maximal performance) were entered into a Mann–Whitney U test for statistical analysis of group differences. A composite TDI (Threshold, Discrimination, Identification) score representing the sum of results obtained by threshold, discrimination, and identification is used to classify olfactory performance, with TDI scores <29 indicating hyposmia, Besides confirming olfactory impairment in PD patients, olfactory tests were used to exclude olfactory dysfunction in controls (also as
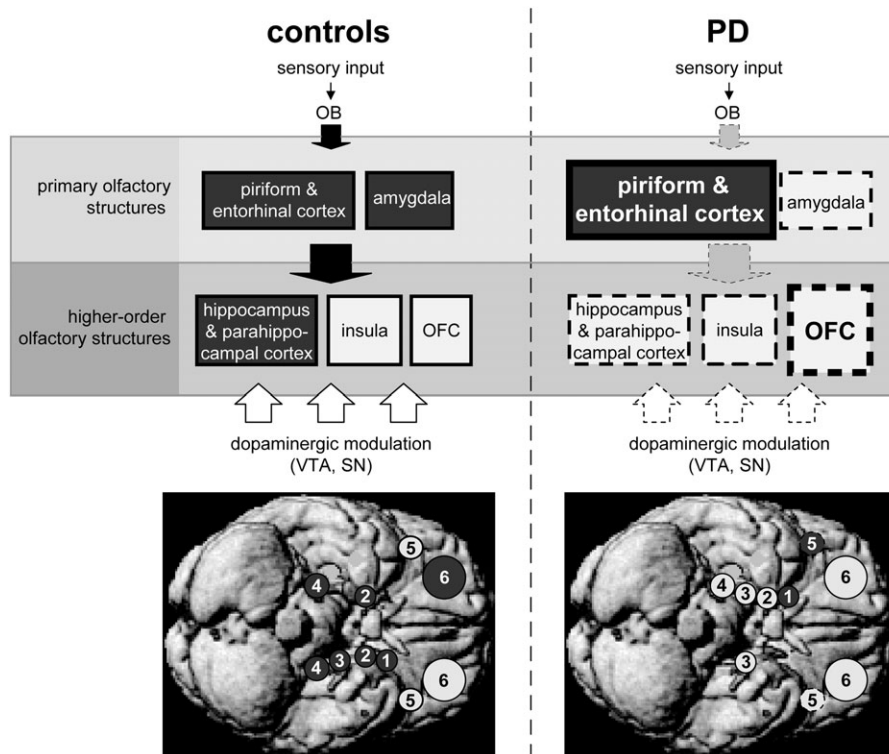
Figure 1. Schematic overview of brain activation in controls (left) and PD patients (right). The physiological network, which is illustrated in the left diagram, was defined on the basis of olfactory-induced brain activation in controls. Olfactory sensory input arrives from the olfactory bulb in primary olfactory structures and is further projected to higher ordered structures (bottom-up processing). The olfactory network is modulated by different neurotransmitters (e.g., dopamine) both at primary and higher order level (top-down modulation). Structures shown on dark background represent core regions of the olfactory network, which emerged exclusively in response to odorant presentation. These include all primary as well as several higher order olfactory structures, most of which are situated in the mesolimbic part of the brain. In contrast, structures shown on bright background, that is, insula and OFC, seem to be target of top-down modulation, as these structures showed significant increase in activation during non-odor events as well. The diseased network in PD patients is shown on the right. Increased size of the boxes indicates hyperactivation. Dashed lines represent a loss of signal–noise discrimination. The degradation of the arrows reflects a hypothesized dysfunction in signal transmission, both bottom-up (projections within the olfactory network, in particular mesolimbic) and top-down (dopaminergic projections of the brain stem). 1: Piriform and entorhinal cortex, 2: amygdala, 3: parahippocampal cortex, 4: hippocampus, 5: insula, and 6: OFC. OB: olfactory bulb, VTA: ventral tegmental area, SN: substantia nigra.

a putative premotor symptom of PD), as well as to confirm remaining ability to discern olfactory stimuli in PD patients.

Odorants and Olfactometry

Olfactory stimuli were presented bilaterally using air-dilution olfactometry. During scanning, subjects wore a common nasal cannula (Airlife, CardinalHealth) consisting of a plastic tube that fits behind the ears, and a pair of prongs that are placed in the nostrils (Ø 2 mm). Besides the advantage of a precise and standardized presentation of the odorants, the nasal cannula minimizes the tendency of the subjects to actively sniff because the airflow is already directed into the nasal cavity.

The following odorants (Sigma-Aldrich) were used at suprathreshold concentration (%): amylacetate (banana, 0.015), ethylbutanol (pineapple, 0.003), and lavender oil (lavender, 0.008). These odorants, which were not identical to any odor used in the Sniffin' Sticks test, have been shown to be predominantly olfactory (Savic et al. 2000; Anderson et al. 2003; Cerf-Ducastel and Murphy 2003). Analysis does not distinguish between the 3 odorants that were used to minimize the effect of desensitization due to adaptation.

Experimental fMRI Design

During the scanning session, subjects were engaged in an odor detection task, which required the differentiation between odor events and blank events (Fig. 2A). Thirty-six odor and 36 blank trials were presented in a pseudorandomized order, with each trial lasting 28 s. Trials were composed of the following phases: baseline (10 s), preparation (2 s), event (10 s), and response (6 s). Subjects were informed about the current phase by the color of a centrally presented

fixation cross. As event phases were separated for at least 18 s, sensory adaptation was minimized. During the response phase, perception of odor in the event phase was indicated via button press, allowing an indirect rating of the subject's olfactory sensitivity in terms of signal detection theory (see below). Before starting the fMRI experiment, subjects were trained to breathe normally and regularly without sniffing.

Imaging Parameters

MR data were obtained with a 3-T Allegra Magnetom (Siemens) equipped with a standard, single-channel, full-head receive coil. A total of 1009 volumes were collected using a T_2^* sensitive echo-planar sequence (echo time [TE]: 30 ms, repetition time [TR]: 2 s, flip angle: 90°, voxel size: $3 \times 3 \times 3$ mm^3, field of view [FOV]: 192 mm, number of slices: 34, slice thickness: 3 mm, slice distance: 0.3 mm, and slice acquisition sequence: interleaved). Slices were oriented slightly oblique to the anterior–posterior commissure plane traversing from frontal pole to temporal pole. After functional data acquisition, a full-brain T_1-weighted 3D image was generated as magnetization-prepared rapid gradient echo (TE: 2.6 ms, TR: 22.50 ms, voxel size: $1 \times 1 \times 1$ mm^3, FOV: 256 mm, and slice thickness: 1 mm).

Behavioral Data Analysis

The button press during MR scanning served as a stimulus-response template for each subject, which could be compared with the actual event of the respective trial. The experiment can therefore be regarded as a typical signal detection situation, which requires a yes–no decision in a noisy environment (Wickens 2002). Trials without olfactory stimulation, that is, blank trials, correspond to noise trials, whereas

trials with olfactory stimulation are called signal (plus noise) trials, referring to the fact that additional information, namely the signal, is superimposed upon the noise. For each subject, the following variables were determined: hit rate h (i.e., ratio of number of hits to number of signal trials), false-alarm rate f (i.e., ratio of number of false alarms to number of noise trials), and sensitivity d'. Parameter estimation for d' was based on the equal-variance Gaussian model, allowing its value to be calculated from h and f:

$$\hat{d}' = Z\left(h\right) - Z\left(f\right).$$

The parameter d' indicates the distance between both noise and signal distributions for each subject. The smaller d', the smaller is the distance, and the more difficult is the discrimination of signal from noise. This parameter therefore approximates the sensitivity of a person. If the value of d' is near 0, the signal cannot be discriminated from noise because both distributions overlap. Detectability increases with increasing d', resulting in a spatial separation of both distributions.

Functional Image Analysis

Image Processing, SPM{T} Extraction, and Contrast Definition
Imaging data were analyzed using SPM5 (Statistical Parametric Mapping, Welcome Trust Centre for Neuroimaging, London, UK). Subsequent to standard spatial preprocessing procedures, including realignment, coregistration, spatial normalization into standard anatomical Montreal Neurological Institute (MNI) space, and smoothing with an 8-mm (full-width half-maximum) Gaussian kernel (Friston et al. 1995), data underwent statistical analysis based on the general linear model. In order to account for transient effects, for example, adaptation (Poellinger et al. 2001), the event phase was split into 2 halves. We were therefore able to model functional activation for the entire 10-s event phase, as well as for the first and the following 5 s of an event. In addition, the response phase was included into the design matrix, resulting in an implicit baseline, which coincides with the baseline phase of the trial. Based on this design matrix, 3 types of contrasts were defined. In "stimulation-specific contrasts," activation during odor events was directly compared with activation during blank events ("odor vs. blank"). In "event-specific contrasts," activation during event phases was compared with baseline ("odor vs. baseline," "blank vs. baseline"). Both stimulation- and event-specific contrasts were analyzed for the entire length of the event, as well as for the first half of the event. Finally, a contrast was computed to selectively assess sensory adaptation, which has been widely documented for primary olfactory areas to occur within 10–30 s after stimulus presentation (Wilson 1998; Sobel et al. 2000; Poellinger et al. 2001; Best and Wilson 2004). Sensory adaptation, also referred to as central habituation, is characterized by a transient increase followed by a prolonged decrease in activation that even falls below baseline level. To optimally model this time course, a "time course–specific contrast" was computed that compares the first half of the event to the second half of each trial ("odor1 vs. odor2," "blank1 vs. blank2").

Experimental Definition of the Olfactory Network
Given the expected variability of the patient sample due to limited accuracy of clinical diagnostic criteria, the olfactory network was defined for subsequent analysis in 2 complementary ways.

As a first approach, activation in controls obtained by random effects analysis was used to define a standard activation pattern that was compared with functional activation in PD patients. This approach allowed for a network definition without being guided by a priori hypotheses. Network definition was conducted based on selectivity patterns of functional activation revealed by the contrasts described above, according to the following rationale: brain regions responding exclusively to one kind of event (i.e., either odor or blank) were classified as "selective," and brain regions reacting to both event types as "unselective." Brain regions selective for odor events can thus be assigned to the olfactory network, which is engaged in bottom-up processing of odorant information. In contrast, selective brain regions

in blank trials appear to be involved in top-down modulation, for example, attention and motivation.

In a second approach, several structurally defined regions of interest (ROI) were selected a priori to approximate the classical olfactory network as reported previously (Savic 2002) to be analyzed in each subject. ROIs were selected from the MNI-based aal database (Tzourio-Mazoyer et al. 2002) implemented in the SPM toolbox MarsBaR (http://marsbar.sourceforge.net) for each hemisphere. Mesolimbic olfactory structures encompass the piriform cortex, amygdala, parahippocampal cortex, and hippocampus. Non-mesolimbic olfactory projection sites include the insula and OFC. To account for functional heterogeneity within the OFC, analysis differentiates among 4 orbitofrontal zones, that is, inferior, superior, medial, and middle OFC. See Supplementary Table s5 for selected ROIs.

Statistical Analysis
1. A voxel-by-voxel analysis was made in terms of whole-brain random effects analysis based on the hemodynamic response function (HRF), both within and between groups, to reveal significant effects of olfactory stimulation without being guided by a priori hypotheses. As clinical populations are generally expected to display a higher heterogeneity in functional activation, group SPM{T}s were thresholded at a more liberal level of $P_{uncorr} < 0.0001$. Only voxels belonging to clusters that surpassed a threshold of $P_{corr} < 0.05$ on cluster level were considered as activated.
2. ROI were analyzed according to 2 different statistical approaches. In order to determine differences in strength of olfactory-induced activation in a priori defined areas, effects of interest were extracted based on a convolution of β parameter estimates with the canonical HRF. Subsequently, mean scores of activation in response to different experimental conditions were calculated for each ROI using the contrasts outlined above. Between-group comparison was conducted on these contrast estimates, and results were reported as being significant at a threshold of $P_{uncorr} < 0.05$ according to nonparametric Mann–Whitney U statistics.
3. In a second approach, time courses of activation based on an alternative model specification (the finite impulse response [FIR] function) were estimated for each ROI and each experimental condition. Significant differences between time courses during odor and blank events indicate the ability of an ROI to discriminate between signal and noise. For this purpose, a mean value as the best representative of a data set was calculated for a time segment, which comprised time points 2-5 after stimulus onset and therefore corresponded to the event phase (seconds 14–20) of the trial. To reveal significant differences in FIR time courses in odor and blank trials within each group, individual mean values of the time segment obtained during odor and blank trials were entered into a Wilcoxon test ($P_{uncorr} < 0.05$).

Results

Behavioral data
Statistical analysis of Sniffin' Sticks scores revealed significantly better performance in controls as compared with PD patients in all 3 subtests of threshold ($Z = 3.274$, $P_{corr} = 0.003$), discrimination ($Z = 2.822$, $P_{corr} = 0.012$), and identification ($Z = 3.916$, $P_{corr} < 0.001$). The mean TDI score in controls was therefore higher and within the normosmic range (mean TDI: 30 + 6, min: 21, max: 37), in contrast to the mean TDI value in PD patients, that showed reduced olfactory function (mean TDI: 19 + 6; min: 13, max: 27). With regard to behavioral performance during scanning, that is, button presses in response to odorant detection, controls were significantly better in identifying olfactory stimuli, that is, signals (h: $Z = 3.783$, $P_{uncorr} = 0.001$), although all PD patients were able to detect all 3 odorants in a test trial before scanning. In contrast,

false alarms were not significantly different between both groups (f: $Z = 1.568$, $P_{uncorr} = 0.119$). Overall signal-noise discrimination (i.e., sensitivity, d') was significantly better in controls (d': $Z = 3.186$, $P_{uncorr} = 0.001$).

fMRI Data

Random Effects Analysis

Selectivity classification of activation in controls was used to define a standard activation pattern that was compared with functional activation in PD patients (Fig. 2B,C and Table 1; for detailed information, see Supplementary Table s2).

Using our paradigm, activated brain regions in controls, which exclusively responded to odor events, correspond to primary olfactory structures (Sobel et al. 2000; Savic 2002) (Fig. 2B). No primary olfactory brain region was active on blank trials. Selective activation in secondary olfactory brain structures was observed in the hippocampus bilaterally, left putamen, and pallidum, as well as left middle and inferior OFC (Brodmann area [BA] 10). Among these olfactory brain regions, habituation, partly with activation falling under baseline level,
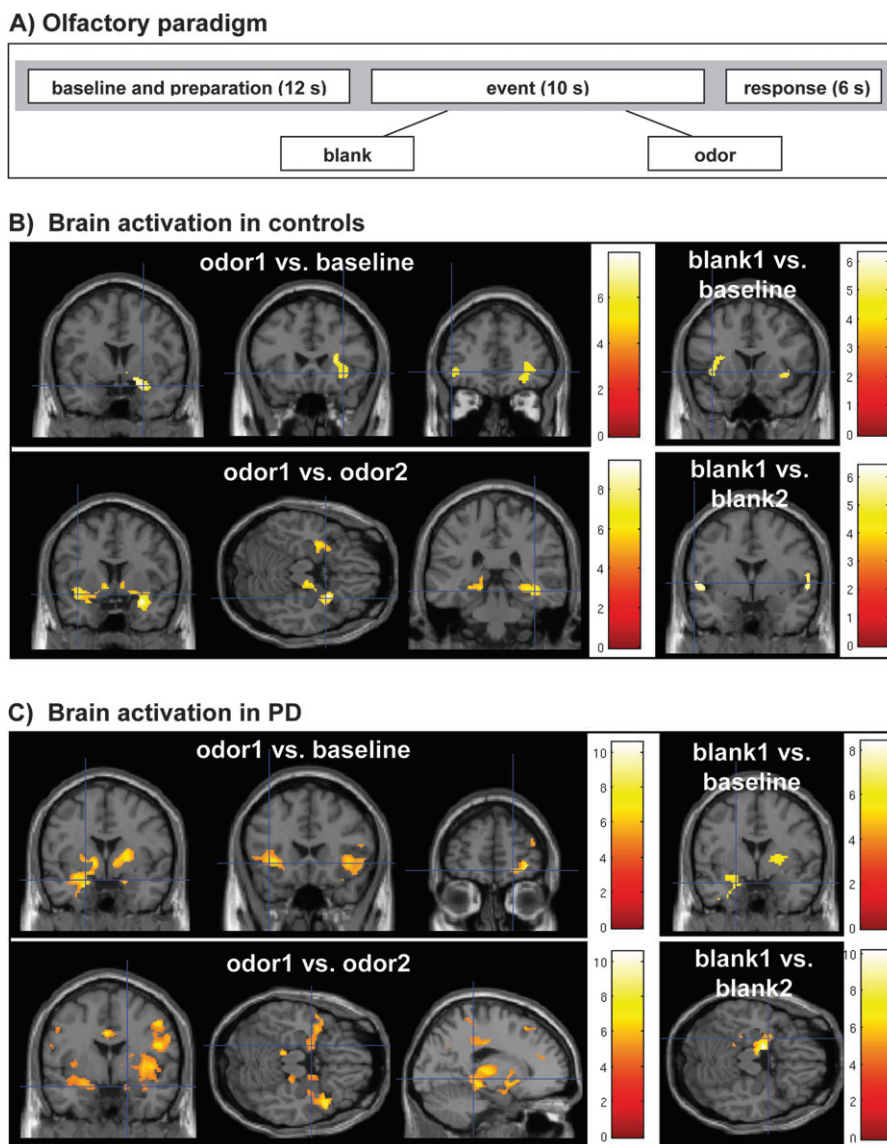
Figure 2. Altered brain activation in PD patients (random effects analysis). (A) Depiction of the experimental time course. Each trial consisted of a baseline, event, and response phase. The only difference between blank and odor trials was the presence or absence of the odorant during event phase. (B and C) Statistical parametric maps showing significant brain activation ($P_{corr} < 0.05$, SPM{T} threshold: $P_{uncorr} < 0.0001$) in controls during odor and blank events, revealed by event-specific contrasts (i.e., comparison of the first half of the event to baseline, "event1 vs. baseline") and time course–specific contrasts (i.e., comparison of the first half of the event to the second half of the same event, "event1 vs. event2"). Depicted activation refers to cross-hair position. (B) Significant activation in controls. "Odor1 vs. baseline": right piriform cortex and amygdala (left; MNI: 26, 4, −18), right insula (middle; MNI: 34, 24, −6), left OFC (right; MNI: −44, 42, −4). "Odor1 vs. odor2": left piriform cortex, amygdala, and superior temporal pole (left; MNI: −38, 6, −12), right amygdala (30, 6, −18), and right hippocampus (right; MNI: 40, −32, −12). "Blank1 vs. baseline": left insula (MNI: −38, 16, −2). "Blank1 vs. blank2": left rolandic operculum and superior temporal gyrus (MNI: −58, 0, 2). (C) Significant activation in PD patients. "Odor1 vs. baseline": right piriform cortex and amygdala (left, MNI: 20, −1, −20), left inferior OFC and insula (middle, MNI: −38, 22, −4), and right superior OFC (right, MNI: 20, 54, −10). "Odor1 vs. odor2": right parahippocampal cortex and amygdala (left, MNI: 18, −1, −18), left amygdala, temporal pole, and middle temporal gyrus (middle, MNI: −20, −1, −18), left hippocampus and thalamus (right, MNI: −20, −34, −2). "Blank1 vs. baseline": left amygdala (MNI: −21, 0, −18). "Blank1 vs. blank2": left piriform cortex, amygdala, and hippocampus (MNI: −17, −3, −18).

could be observed in the piriform cortex, parahippocampal cortex, and in the hippocampus, as revealed by the time-course–specific contrast. In contrast, unselective activation during both odor and blank events was displayed in the insula bilaterally and in the right middle and inferior OFC (BA 11).

In PD patients, the difficulty to discern between olfactory stimuli is reflected in the reduced selectivity of brain activation in response to olfactory stimulation. Only the left piriform cortex (part of the primary olfactory cortex) and insula (part of the secondary olfactory cortex) showed selective activation in odor trials, while the remaining primary and secondary olfactory structures displayed a significant, unselective increase in activation (e.g., amygdala, hippocampus, parahippocampal, and OFC, Fig. 2C). In addition, those brain regions that were selective for blank events in controls were also activated during odor events in PD patients, that is, amygdala, hippocampus, and left OFC.

Direct between-group comparison was statistically too restrictive to obtain significant results, which can also be attributed to susceptibility artifacts in mesial brain regions, and to activation differences between both groups, which are not pronounced enough to survive statistical whole-brain correction.

ROI Analysis

Differences in activation strength. When directly comparing functional activation between controls and PD patients in predefined ROIs, statistically significant differences can be found in
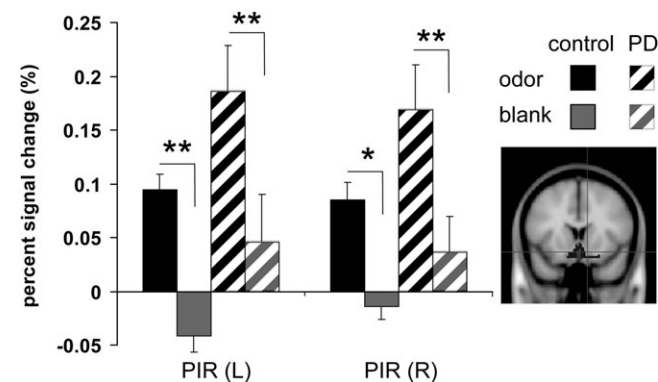
the piriform cortex as the main part of the primary olfactory cortex and in orbitofrontal areas due to hyperactivation in PD patients (see Supplementary Table s3 and Fig. s1). No hyperactivation was observed in the remaining parts of the olfactory network, that is, amygdala, insula, hippocampus, and parahippocampal cortex.

In accordance with results obtained by random effects analysis indicating a loss of selectivity of the olfactory network, hyperactivation of the piriform and OFC was observed during both odor and blank trials. However, a closer look on the hyperactivation of the piriform cortex revealed significantly different levels of activation during odor and blank trials, suggesting preserved selectivity to odor trials despite a general increase of activation (Fig. 3). This question is further explored using FIR-based analysis of time courses.

Differences in activation time course. When FIR time courses of odor (i.e., signal) trials were compared with those of blank (i.e., noise) trials, between-group comparison revealed reduced discriminatory ability in PD patients, thereby confirming the loss of selectivity as well as the behavioral results obtained in signal detection analysis (see Supplementary Tables s4 and s5). Signal-noise discrimination was evident in only 6 ROIs in PD patients, whereas controls showed selectivity for olfactory stimulation in 9 ROIs. This difference is mainly due to a lack of signal-to-noise discrimination in orbitofrontal regions, which fits the results obtained by HRF-based ROI analysis indicating hyperactivation. Interestingly, the hyperactivated piriform cortex sustains discriminatory ability, thereby confirming the findings of both random effects and HRF-based ROI analysis. Detailed comparison of both groups reveals a loss of selectivity in the left amygdala (Fig. 4A,B), right hippocampus (Fig. 4C,D), and in the OFC bilaterally in PD patients.

Discussion

In the present study, we could identify significant alterations within the olfactory network in PD (Fig. 1), including hyperactivation and reduced signal-noise discrimination. Alterations could be found at various levels of the cerebral olfactory

Table 1

Significant brain activation in controls and PD patients during odor and blank (i.e., non-odor) events as revealed by random effects, classified according to selectivity

Odor trials		Blank trials
Controls		
Selective	Unselective	Selective
Piriform (R)	Insula (L, R)	Rolandic operculum (L, R)
Amygdala (L, R)	Precuneus (L)	Superior temporal gyrus (L, R)
Parahippocampal (R)	Postcentral gyrus (L)	Middle temporal gyrus (L)
Hippocampus (L, R)	Middle OFC (R)	Cuneus (L, R)
Superior temporal pole (L, R)	Inferior OFC (R)	Middle cingulate gyrus (R)
Putamen (L)		Superior frontal gyrus (R)
Pallidum (L)		Inferior frontal operculum (L)
Middle OFC (L)		
Inferior OFC (L)		
PD patients		
Selective	Unselective	Selective
Piriform (L)	Amygdala (L)	Middle temporal gyrus (L)
Pallidum (L)	Parahippocampal (L, R)	
Insula (L)	Hippocampus (L)	
Middle temporal gyrus (R)	Superior temporal pole (L, R)	
Superior temporal gyrus (L, R)	Insula (R)	
	Middle OFC (L, R)	
	Inferior OFC (L, R)	
	Anterior cingulate gyrus (R)	
	Putamen (L, R)	
	Precuneus (L, R)	
	Postcentral gyrus (L, R)	
	Rolandic operculum (L)	
	Inferior frontal operculum (L, R)	

Note: Brain activation revealed by the 3 HRF-based contrast estimations (i.e., stimulation-specific, event-specific, and time course–specific contrast) was classified in terms of selectivity, thereby allowing a characterization of altered activation patterns in PD as compared with the activation pattern shown by controls (i.e., standard activation pattern). For detailed information, see Supplementary Table s2. L = left and R = right.

Figure 3. Preserved olfactory discrimination in the hyperactivated piriform cortex in PD (ROI analysis). When comparing odor events to blank events, signal–noise discrimination as shown in controls (full bars) persists in PD patients (striped bars). However, a general hyperactivation to both events can be found in PD patients. Mean percent signal change + standard error (averaged over time bins 2–5, i.e., seconds 2–10) of the left and right piriform cortex (PIR) in controls and PD patients (PD) during odor and blank events, with $**P_{uncorr} < 0.01$, $*P_{uncorr} < 0.05$, according to nonparametric Wilcoxon statistic.
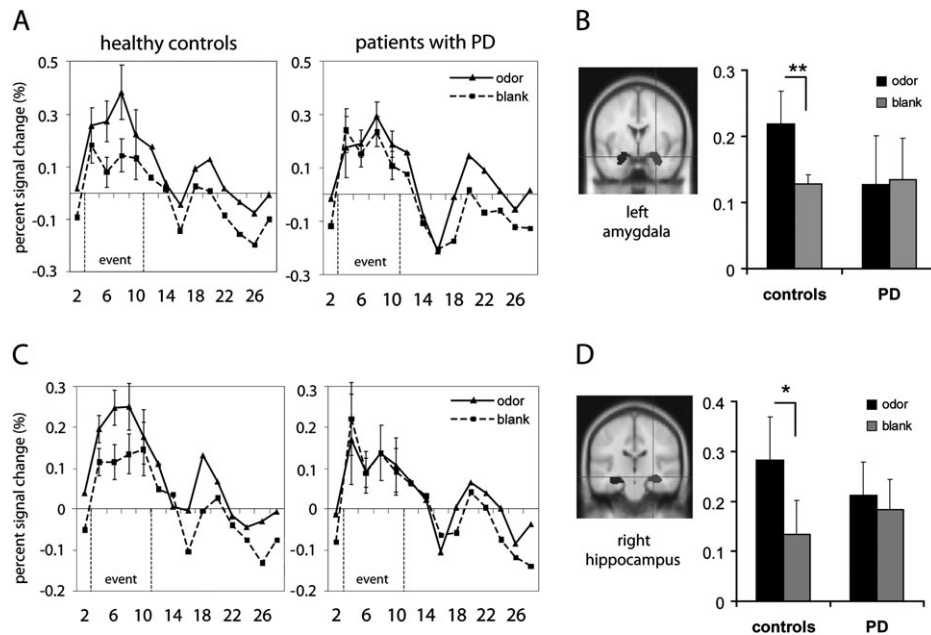
Figure 4. Loss of signal–noise discrimination in the olfactory network in PD (ROI analysis). (*A* and *C*) FIR time courses during odor and blank trials (mean percent signal change of each single time bin ± standard error [SE]) in controls (left) and PD patients (right) in the left amygdala (*A*) and right hippocampus (*C*). The highlighted area represents the event phase (seconds 2–10 after stimulus onset, i.e., odor presentation) of the trial. The axis of ordinates is depicted in seconds. (*B* and *D*) Mean percent signal change ± SE, averaged over time bins 2–5, that is, seconds 2–10, in the left amygdala (*B*) and right hippocampus (*D*), with **$P_{uncorr} < 0.01$, *$P_{uncorr} < 0.05$, according to nonparametric Wilcoxon statistic.

system, as revealed by both random effects and ROI analysis, which are 2 complementary approaches chosen to obtain a detailed picture of functional olfactory activation in PD. Importantly, the piriform cortex, which is considered as the major part of the primary olfactory cortex receiving direct input from the olfactory bulb, displays pronounced hyperactivation in PD patients, but at the same time is significantly modulated by the presence of olfactory stimulation. This sets it apart from higher order structures of the olfactory network that have lost their ability to distinguish signal from noise and bears important implications with regard to the role of early and pronounced pathological affection of the bulb hypothetically causing olfactory deficits in PD.

Hyperactivation at All Levels of the Olfactory System

Contrary to our original hypothesis of a degeneration-induced hypoactivation in directly affected mesolimbic olfactory structures, this study provides evidence for a profound hyperactivation of the olfactory network. At best, the only hint for PD-related hypoactivation is the reduced recruitment of right-hemispheric olfactory brain regions, which was indicated in the statistically restrictive whole-brain random effects analysis. Likewise, a previous study reported unilateral, left-sided activation of the amygdala and hippocampus comparing whole-brain random effects between controls and patients (Westermann et al. 2008). However, whereas this study focused on dopaminergic modulated brain regions related to corticostriatal loops, we further explored regions representing core units of the olfactory system, thereby revealing profound hyperactivation in both left and right hemispheric olfactory centers. This implies that PD-related pathology, at least in early stages of the disease, does not lead to a reduction in neuronal activity in directly affected brain regions, but rather has an opposite effect on activation level. A follow-up study did not

report increased, but rather decreased activation in primary and secondary olfactory structures for patients with disturbed olfactory event-related potentials (OERPs) (Welge-Lussen et al. 2009) suggesting that reduced integrity of signal transmission as reflected by OERPs (Lotsch and Hummel 2006) is associated with advanced neurodegeneration. Combining these findings with the results of the present study, a complex pattern of olfactory network dysregulation in PD emerges, presumably including both bottom-up and top-down processes. These may relate to 1) disrupted signal transmission as a direct effect of neurodegeneration within early olfactory structures, 2) alterations in modulation of neuroplasticity within olfactory information processing, and 3) disease stage-dependent changes in dysregulation patterns. Intriguingly, hyperactivation in PD patients has also been reported in response to motor stimuli (for reviews, see Dagher and Nagano-Saito 2007), within core regions of the motor network such as sensorimotor cortices (Sabatini et al. 2000; Haslinger et al. 2001; Muller et al. 2003; Yu et al. 2007), as well as in functionally related motor networks (Samuel et al. 1997; Catalan et al. 1999; Haslinger et al. 2001). These changes in activation might result not only directly from detrimental disinhibition due to dopamine deficiency, which presumably relates to specific motor symptoms such as rigidity and bradykinesia (Kleine et al. 2001; Pierantozzi et al. 2001) but also from compensatory upregulation (Sabatini et al. 2000; Ceballos-Baumann 2003). Although the present data cannot be directly compared with results obtained in these studies, similar considerations could be addressed for the olfactory network as well. Thus, neurodegeneration-based loss of signal transmission and/or compensatory mechanisms might contribute to hyperactivation associated with olfactory dysfunction. Considering the finding that hyperactivation seems to be limited to the initial input stage of the cerebral olfactory network, namely the piriform cortex and the OFC that can be

seen as an higher order convergence zone of top-down and bottom-up processes, we propose that the network's core unit (primary olfactory structures) displays dysfunctional disinhibition due to early pathology and/or dopaminergic depletion, which subsequently leads to compensatory activation in functionally related, higher order units of the network.

Preserved Olfactory Discrimination in the Piriform Cortex in PD

All statistical approaches, in particular ROI analysis based on the FIR function, revealed a profound loss of signal–noise discrimination in the olfactory system of PD patients. However, while secondary structures, including amygdala, hippocampus, and orbitofrontal areas lost their ability to discriminate signal from noise (Fig. 1), the piriform cortex in the hyposmic PD patients is still able to isolate olfactory input. Thus, the crucial loss of information during olfactory signal propagation leading to hyposmia in PD patients is not only limited to impaired signal propagation by the olfactory bulb and tract. Extensive pathology affecting both neurites (Lewy neurites) and neuronal cell bodies (Lewy bodies) is found in the olfactory bulb and anterior olfactory nucleus in early PD (Braak et al. 2002), which is accompanied by a substantial increase in dopaminergic inhibitory interneurons in the olfactory bulb (Huisman et al. 2004, 2008), and disrupted olfactory tract fibers (Scherfler et al. 2006). These studies suggest that loss of signal input is caused by structural alterations in the olfactory bulb and tract. Further evidence of atrophy in olfactory brain regions links impaired sensory processing to structural decline (Wattendorf et al. 2009). Thus, neurodegeneration-mediated disinhibition might cause hyperactivation. However, in light of the present functional data and recent neuropathological finding describing heterogeneous pathological affection of the piriform cortex (Silveira-Moriyama et al. 2009), hyperactivation of the piriform cortex seems to indicate the distortion of olfactory information when being propagated to higher order units of the olfactory network. However, the persistent ability of the primary olfactory cortex to discriminate between signal and noise supports the hypothesis that olfactory impairment in PD is not only limited to loss of signal input from pathologically affected olfactory bulb and tract, but functional impairment of the entire olfactory system is relevant for hyposmia in PD.

Having characterized distinct activation patterns within the olfactory network in PD in this study, the question regarding its specificity compared with other hyposmic patients has to be addressed in further research. To date, only few studies have investigated functional activation to odors in hyposmia of different etiologies (congenital hyposmia, Henkin and Levy 2002, Alzheimer's disease, Wang et al. 2010, and various etiologies other than neurologic/psychiatric, Levy et al. 1998). To our knowledge, none of these studies has reported hyperactivation in response to olfactory stimulation. In contrast, volumetric analysis of MR data has revealed reduced gray matter volume in a wide range of hyposmics, for example, in PD (Wattendorf et al. 2009), Alzheimer's disease (Thomann et al. 2009), genetic aberrations (Blustajn et al. 2008), and posttraumatic hyposmia (Collet et al. 2009; Bitter et al. 2010). Thus, future comparative analyses are required to determine PD-specific structural and functional alterations associated with hyposmia.

The present study offers new insights into neural plasticity within disturbed functional networks in early PD in order to restore performance. The observed hyperactivation suggests compensatory upregulation of neural activity at all levels of olfactory information processing. However, the observed loss of signal-to-noise discrimination in mesolimbic olfactory structures, which appears to be spread to higher-order regions of the olfactory network, indicates the failure of this compensatory attempt. Moreover, we propose that impairment of olfactory network function is a dynamic process during the course of PD, which might be used to identify different stages of the disease process in PD. Our findings extend the knowledge of altered activation patterns of the olfactory system in PD patients (Fig. 1). In conjunction with previous approaches to correlate olfactory dysfunction in at-risk populations of PD (Ponsen et al. 2004; Sommer et al. 2004; Stiasny-Kolster et al. 2005), our results with respect to changes in the neural circuitry associated with PD underline the importance of understanding olfactory dysfunction to provide ground for establishing additional diagnostic tools for early premotor PD.

Supplementary Material

Funding

Notes

References

Anderson AK, Christoff K, Stappen I, Panitz D, Ghahremani DG, Glover G, Gabrieli JD, Sobel N. 2003. Dissociated neural representations of intensity and valence in human olfaction. Nat Neurosci. 6:196–202.

Beck AT, Ward C, Mendelson M. 1961. Beck Depression Inventory (BDI). Arch Gen Psychiatry. 4:561–571.

Best AR, Wilson DA. 2004. Coordinate synaptic mechanisms contributing to olfactory cortical adaptation. J Neurosci. 24:652–660.

Bitter T, Brüderle J, Gudziol H, Burmeister HP, Gaser C, Guntinas-Lichius O. 2010. Gray and white matter reduction in hyposmic subjects—a voxel-based morphometry study. Brain Res. 1347:42–47.

Blustajn J, Kirsch CFE, Panigrahy A, Netchine I. 2008. Olfactory anomalies in CHARGE syndrome: imaging findings of a potential major diagnostic criterion. Am J Neuroradiol. 29:1266–1269.

Braak H, Del Tredici K, Bratzke H, Hamm-Clement J, Sandmann-Keil D, Rub U. 2002. Staging of the intracerebral inclusion body pathology associated with idiopathic Parkinson's disease (preclinical and clinical stages). J Neurol. 249:1–5.

Braak H, Ghebremedhin E, Rub U, Bratzke H, Del TK. 2004. Stages in the development of Parkinson's disease-related pathology. Cell Tissue Res. 318:121–134.

Catalan MJ, Ishii K, Honda M, Samii A, Hallett M. 1999. A PET study of sequential finger movements of varying length in patients with Parkinson's disease. Brain. 122:483–495.

Ceballos-Baumann AO. 2003. Functional imaging in Parkinson's disease: activation studies with PET, fMRI and SPECT. J Neurol. 250:I15–I23.

Cerf-Ducastel B, Murphy C. 2003. FMRI brain activation in response to odors is reduced in primary olfactory areas of elderly subjects. Brain Res. 986:39–53.

Collet S, Grulois V, Bertrand B, Rombaux P. 2009. Post-traumatic olfactory dysfunction: a cohort study and update. B-ENT. 5:97–107.

Dagher A, Nagano-Saito A. 2007. Functional and anatomical magnetic resonance imaging in Parkinson's disease. Mol Imaging Biol. 9:234–242.

Doty RL. 2008. The olfactory vector hypothesis of neurodegenerative disease: is it viable? Ann Neurol. 63:7–15.

Fahn JJ, Elton R. 1987. The Unified Parkinson's disease rating scale. Fahn S, Marsden CD, Calne DB, Goldstein M, editors. Recent developments in Parkinson's disease. Florham Park (NJ): Macmillan Health Care Information. p.153–163, 293–304.

Folstein MF, Folstein SE, McHugh PR. 1975. "Mini-mental state". A practical method for grading the cognitive state of patients for the clinician. J Psychiatr Res. 12:189–198.

Friston KJ, Frith CD, Frackowiak RS, Turner R. 1995. Characterizing dynamic brain responses with fMRI: a multivariate approach. Neuroimage. 2:166–172.

Gelb DJ, Oliver E, Gilman S. 1999. Diagnostic criteria for Parkinson disease. Arch Neurol. 56:33–39.

Haslinger B, Erhard P, Kampfe N, Boecker H, Rummeny E, Schwaiger M, Conrad B, Ceballos-Baumann AO. 2001. Event-related functional magnetic resonance imaging in Parkinson's disease before and after levodopa. Brain. 124:558–570.

Henkin RI, Levy LM. 2002. Functional MRI of congenital hyposmia: brain activation to odors and imagination of odors and tastes. J Comput Assisted Tomogr. 26:39–61.

Hoehn MM, Yahr MD. 2001. Parkinsonism: onset, progression, and mortality. 1967. Neurology. 57:S11–S26.

Huisman E, Uylings HB, Hoogland PV. 2004. A 100% increase of dopaminergic cells in the olfactory bulb may explain hyposmia in Parksinson's disease. Mov Disord. 12:687–692.

Huisman E, Uylings HB, Hoogland PV. 2008. Gender-related changes in increase of dopaminergic neurons in the olfactory bulb in Parkinson's disease patients. Mov Disord. 23:1407–1413.

Kleine BU, Praamstra P, Stegeman DF, Zwarts MJ. 2001. Impaired motor cortical inhibition in Parkinson's disease: motor unit responses to transcranial magnetic stimulation. Exp Brain Res. 138:477–483.

Kobal G, Hummel T, Sekinger B, Barz S, Roscher S, Wolf S. 1996. "Sniffin' sticks": screening of olfactory performance. Rhinology. 34:222–226.

Levy LM, Henkin RI, Hutter A, Lin CS, Schellinger D. 1998. Mapping brain activation to odorants in patients with smell loss by functional MRI. J Comput Assisted Tomogr. 22:96–103.

Lotsch J, Hummel T. 2006. The clinical significance of electrophysiological measures of olfactory function. Behav Brain Res. 170:78–83.

Muller JL, Deuticke C, Putzhammer A, Roder CH, Hajak G, Winkler J. 2003. Schizophrenia and Parkinson's disease lead to equal motor-related changes in cortical and subcortical brain activation: an fMRI fingertapping study. Psychiatry Clin Neurosci. 57:562–568.

Palop JJ, Chin J, Mucke L. 2006. A network dysfunction perspective on neurodegenerative diseases. Nature. 443:768–773.

Pierantozzi M, Palmieri MG, Marciani MG, Bernardi G, Giacomini P, Stanzione P. 2001. Effect of apomorphine on cortical inhibition in Parkinson's disease patients: a transcranial magnetic stimulation study. Exp Brain Res. 141:52–62.

Poellinger A, Thomas R, Lio P, Lee A, Makris N, Rosen BR, Kwong KK. 2001. Activation and habituation in olfaction–an fMRI study. Neuroimage. 13:547–560.

Ponsen MM, Stoffers D, Booij J, van Eck-Smit BL, Wolters EC, Berendse HW. 2004. Idiopathic hyposmia as a preclinical sign of Parkinson's disease. Ann Neurol. 56:173–181.

Sabatini U, Boulanouar K, Fabre N, Martin F, Carel C, Colonnese C, Bozzao L, Berry I, Montastruc JL, Chollet F, et al. 2000. Cortical motor reorganization in akinetic patients with Parkinson's disease: a functional MRI study. Brain. 123:394–403.

Samuel M, Ceballos-Baumann AO, Blin J, Uema T, Boecker H, Passingham RE, Brooks DJ. 1997. Evidence for lateral premotor and parietal overactivity in Parkinson's disease during sequential and bimanual movements. A PET study. Brain. 120:963–976.

Savic I. 2002. Imaging of brain activation by odorants in humans. Curr Opin Neurobiol. 12:455–461.

Savic I, Gulyas B, Larsson M, Roland P. 2000. Olfactory functions are mediated by parallel and hierarchical processing. Neuron. 26:735–745.

Scherfler C, Schocke MF, Seppi K, Esterhammer R, Brenneis C, Jaschke W, Wenning GK, Poewe W. 2006. Voxel-wise analysis of diffusion weighted imaging reveals disruption of the olfactory tract in Parkinson's disease. Brain. 129:538–542.

Silveira-Moriyama L, Holton JL, Kingsbury A, Ayling H, Petrie A, Sterlacci W, Poewe W, Maier H, Lees AJ, Revesz T. 2009. Regional differences in the severity of Lewy body pathology across the olfactory cortex. Neurosci Lett. 453:77–80.

Sobel N, Prabhakaran V, Zhao Z, Desmond JE, Glover GH, Sullivan EV, Gabrieli JD. 2000. Time course of odorant-induced activation in the human primary olfactory cortex. J Neurophysiol. 83:537–551.

Sommer U, Hummel T, Cormann K, Mueller A, Frasnelli J, Kropp J, Reichmann H. 2004. Detection of presymptomatic Parkinson's disease: combining smell tests, transcranial sonography, and SPECT. Mov Disord. 19:1196–1202.

Stiasny-Kolster K, Doerr Y, Moller JC, Hoffken H, Behr TM, Oertel WH, Mayer G. 2005. Combination of 'idiopathic' REM sleep behaviour disorder and olfactory dysfunction as possible indicator for alpha-synucleinopathy demonstrated by dopamine transporter FP-CIT-SPECT. Brain. 128:126–137.

Thomann PA, Dos Santos V, Seidl U, Toro P, Essig M, Schröder J. 2009. MRI-derived atrophy of the olfactory bulb and tract in mild cognitive impairment and Alzheimer's disease. J Alzheimers Dis. 17:213–221.

Tzourio-Mazoyer N, Landeau B, Papathanassiou D, Crivello F, Etard O, Delcroix N, Mazoyer B, Joliot M. 2002. Automated anatomical labeling of activations in SPM using a macroscopic anatomical parcellation of the MNI MRI single-subject brain. Neuroimage. 15:273–289.

Wang J, Eslinger PJ, Doty RL, Zimmerman EK, Grunfeld R, Sun X, Connor JR, Price JL, Smith MB, Yang QX. 2010. Olfactory deficit detected by fMRI in early Alzheimer's disease. Brain Res. doi:10.1016/j.brainres.2010.08.018.

Wattendorf E, Welge-Lussen A, Fiedler K, Bilecen D, Wolfensberger M, Fuhr P, Hummel T, Westermann B. 2009. Olfactory impairment predicts brain atrophy in Parkinson's disease. J Neurosci. 29:15410–15413.

Welge-Lussen A, Wattendorf E, Schwerdtfeger U, Fuhr P, Bilecen D, Hummel T, Westermann B. 2009. Olfactory-induced brain activity in Parkinson's disease relates to the expression of event-related potentials: a functional magnetic resonance imaging study. Neuroscience. 162:537–543.

Westermann B, Wattendorf E, Schwerdtfeger U, Husner A, Fuhr P, Gratzl O, Hummel T, Bilecen D, Welge-Lussen A. 2008. Functional imaging of the cerebral olfactory system in patients with Parkinson's disease. J Neurol Neurosurg Psychiatr. 79:19–24.

Wickens TD. 2002. Elementary signal detection theory. Oxford: Oxford University Press.

Wilson DA. 1998. Habituation of odor responses in the rat anterior piriform cortex. J Neurophysiol. 79:1425–1440.

Yu H, Sternad D, Corcos DM, Vaillancourt DE. 2007. Role of hyperactive cerebellum and motor cortex in Parkinson's disease. Neuroimage. 35:222–233.

Zaccai J, Brayne C, McKeith I, Matthews F, Ince PG. 2008. Patterns and stages of alpha-synucleinopathy: relevance in a population-based cohort. Neurology. 70:1042–1048.